

## An Empirical Procedure to Estimate Distances to Stellar Clusters

Carlos Allende Prieto

*McDonald Observatory and Department of Astronomy, The University of Texas at Austin, Texas  
78712-1083*

callende@astro.as.utexas.edu

### ABSTRACT

A most desirable feature of a standard candle to estimate astronomical distances is robustness against changes in metallicity and age. It is argued that the radii of main sequence stars with spectral types from solar to A0 show predictable changes with metallicity, and detectable changes with evolution. Such stars populate the solar neighborhood, and therefore benefit from measurements of angular diameters. Also, reliable determinations of their masses and radii are available from observations of eclipsing binaries. Three empirical relationships are defined and suggested for estimating distances to dwarfs from only *BVK* photometry. Comparison with *Hipparcos* trigonometric parallaxes shows that the method provides errors of about 15 % for a particular star, which can be reduced to roughly 1.5 % when applied to young clusters (age  $\lesssim 1 - 2$  Gyr) with  $\sim 100$  stars of the appropriate spectral types. If reddening is unknown, main sequence stars with effective temperatures close to 8000 K can constrain it, although an estimate of  $\mathcal{R} \equiv A(V)/E(B - V)$  is required.

*Subject headings:* Galaxy: open clusters and associations: general — stars: distances — stars: fundamental parameters

### 1. Introduction

Reliable distance estimators are scarce, yet required for many purposes. A few examples will suffice here. Spectroscopic parallaxes are typically used to estimate distances to massive stars across the Galaxy (e.g. Reed & Reed 2000) for the lack of a better tool. Astrometric parallaxes are usually in need of distance estimates for reference stars very close in the sky to the main target (see, e.g., McArthur et al. 1999). Again, spectroscopic classification and *standard* brightness expectations are combined to yield a distance. Accurate distances to clusters derived independently from stellar evolution models are key to test both the models and cluster ages inferred for them (Rosenberg et al. 1999). The *Hipparcos* mission (ESA 1997) has greatly improved the situation on this front, with

very precise mean parallaxes for nearby clusters (Robichon et al. 1999), but a discussion on possible systematic errors for some clusters is still open (see Pinsonneault et al. 1998). Finally, the Hubble Space Telescope Key Project’s effort to constrain the value of the Hubble’s constant from different standard candles relies on the cepheids period-luminosity relationship, which is itself based on the assumed distance to the Large Magellanic Cloud and mainly limited in accuracy by its uncertainty (Mould et al. 2000). Different methods of deriving that distance have been implemented, and have been recently critically reviewed by Feast (1999): pulsating stars, supernovae, red-clump stars, and eclipsing binaries have been proposed. The situation is worrying, as the different estimates span a range of a 30%.

A desirable virtue of a procedure to estimate distances is robustness against systematic errors. Most distance estimators rely on relationships between observed quantities and fundamental properties of the standard objects employed. Then, one of the main goals is to understand how the properties of the standard object change with possible parameters, typically metal content and age. This is possible for any kind of star, based on an appropriate understanding of stellar structure and evolution, but maximizing simplicity reduces the uncertainties. State-of-the-art stellar interior models provide an extraordinary guide, but the complexity of the physics, and the difficulties in relating observed and fundamental parameters make them of limited accuracy to derive distances.

Some basic quantities are within reach from direct measurements for nearby objects: parallaxes and angular diameters. However, nearby means here roughly a hundred parsecs for the parallax (see the *Hipparcos* Catalogue) and, highly dependent on the stellar radius, from several tens to a few hundreds of parsecs for the angular diameter (see, e.g., van Belle 1999). More interesting stellar properties, masses and radii, can be directly determined from combined spectroscopic and photometric observations of double-lined eclipsing binaries (see, e.g., Andersen 1991). Some of such systems are indeed close enough to have highly accurate parallaxes, providing additional information (Ribas et al. 1998; Popper 1998). As a result of the distribution of mass and brightness of the stellar population of the solar neighborhood, the most direct measurements of parallaxes, angular diameters, radii, and masses, involve main-sequence stars with masses between one and three times larger than solar. These stars should be preferred to derive empirical relationships between their physical parameters and measurements, and are proposed here for deriving distances to stellar clusters.

## 2. Description of the proposed method

The suggested recipe is a kind of *photometric parallax*. First, it is possible to use a Barnes-Evans like relationship between the surface brightness and a color index to estimate stellar angular diameters from photometric measurements. A second empirical relation between the stellar radius and a color index, or the absolute magnitude, constrains the radius and, when reddening is absent or well known, fixes the distance. At least in theory, a third equation would close the system, allowing for the amount of reddening to be determined.

## 2.1. Known reddening

The surface brightness, defined as  $S_V = 15 + V_0 + 5 \log \theta$ , where  $V_0$  is the Johnson V magnitude and  $\theta$  is the stellar angular diameter in arcseconds, has been shown by Di Benedetto (1998) to follow a tight correlation with the  $(V - K)_0$  color index. This is understandable because (1)  $S_V$  is linearly related with the bolometric correction and the logarithm of the stellar effective temperature ( $T_{\text{eff}}$ ), and (2) the  $(V - K)_0$  broad-band color index is almost insensitive to any stellar parameter other than  $T_{\text{eff}}$  (Wesselink 1969, Barnes & Evans 1976). Di Benedetto fitted a second-order polynomial to the observed  $S_V$  as a function of  $(V - K)_0$  for nine dwarfs and subgiants, finding a scatter in the fit of 0.03 mag for the range  $-0.1 \leq (V - K)_0 \leq 1.5$  (spectral types  $\sim$  A0–G2). This relationship binds the stellar radius and the distance to the star in a very solid manner. The relationship remains almost the same as stars evolve away from the main sequence. Besides, model atmospheres and stellar evolutionary models predict it to hold for any metallicity.

Figure 1 shows the data and the polynomial fitted by Di Benedetto (solid line). The predictions from the isochrones of Bertelli et al. (1994) with ages from 4 Myr up to 20 Gyr and metallicities ( $Z$ ) from 0.004 to 0.05 have been over-plotted with different line styles and lay on top of the fit for  $0.5 \lesssim (V - K)_0 \lesssim 1.5$ , but predict a slightly lower surface brightness for bluer colors. Di Benedetto excluded two stars from the fit ( $\alpha$  Aql and  $\beta$  Car). The star  $\alpha$  Aql is clearly off the correlation, but one might argue whether  $\beta$  Car or the evolved  $\alpha$  Oph should be excluded or not. Including or excluding any of those stars, the coefficients of the fitting polynomial do not change significantly, and for this reason we have adopted those published by Di Benedetto:

$$S_V = 2.556 + 1.580(V - K)_0 - 0.106(V - K)_0^2 \text{ mag}, \quad (1)$$

which is valid in the range  $-0.1 \leq (V - K)_0 \leq 1.5$ , and shows a scatter of 0.03 mag. Van Belle (1999) has carried out an equivalent regression between the zero-magnitude angular sizes and the  $(V - K)_0$  colors that can be translated to the dashed line in Figure 1. His figures are inconsistent with Di Benedetto's, in particular for the Sun.

The  $S_V$  vs.  $(V - K)_0$  relationship allows us to estimate the angular diameter of the star ( $\theta$ ) and, consequently, relate the stellar radius with the distance to, or the parallax ( $p$ ) of, the star:

$$\log \frac{R}{R_\odot} = 2.031 + \log \theta - \log p, \quad (2)$$

where  $\theta$  and  $p$  are in arcseconds, and it has been used that 1 pc is approximately  $3.086 \times 10^{16}$  m, and  $R_\odot \simeq 6.960 \times 10^8$  m.

A second relationship is required to break the ambiguity between distance and radius. The list of eclipsing binaries compiled by Andersen (1991) can be used to empirically identify the link between radius and absolute visual magnitude for main sequence stars, as shown in Figure 2. The

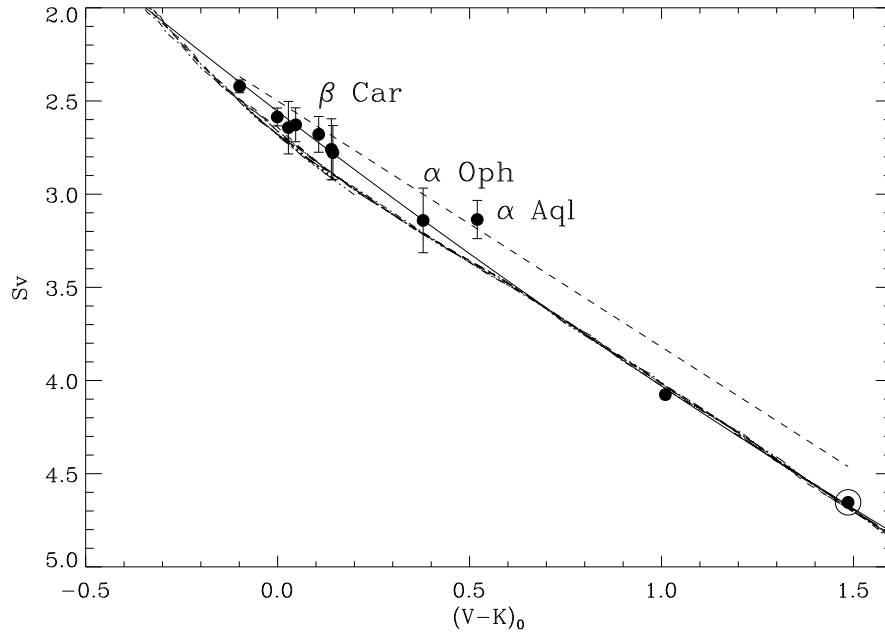


Fig. 1.— Relationship between the surface brightness ( $S_V$ ) and the  $(V - K)_0$  color index for the ten dwarfs and subgiants (plus a giant,  $\alpha$  Oph), and the polynomial fit derived by Di Benedetto (1998; solid line). The dashed line corresponds to the relationship between the  $V$  zero-magnitude and the  $(V - K)_0$  color derived by van Belle (1999), and all the other curves show the predictions of the isochrones of Bertelli et al. (1994) for different metallicities and ages (see text). The Sun is identified by the usual symbol ( $\odot$ ).

list has been supplemented with the systems RT And and CG Cyg (Popper 1994), as they fill an important gap at masses slightly larger than solar. As the stellar radius increases along with the stars' evolution during its main sequence phase, we are interested in narrowing the range of radii as much as possible. The evolution from the Zero Age Main Sequence (ZAMS) can be constrained from the extremely accurate gravities available for these stars. From the stars spectroscopically classified as dwarfs in Andersen's list, I have retained only those whose gravities were not lower than 23 % (0.1 dex) of the value predicted at the ZAMS by the isochrones. In Figure 2, the stars included in the fit are identified with filled circles and error bars, while those not included are represented by crosses. The least-squares fit (solid line) is

$$\log \frac{R}{R_\odot} = 3.820 \times 10^{-1} - 9.801 \times 10^{-2} M_V + 7.636 \times 10^{-3} M_V^2 + 4.895 \times 10^{-4} M_V^3 - 6.133 \times 10^{-5} M_V^4 - 2.831 \times 10^{-5} M_V^5, \quad (3)$$

holds for  $-4.6 \leq M_V \leq 5.7$ , and exhibits a standard deviation of 0.02 dex.

The isochrones with ages younger than  $\sim 1$  Gyr (dashed, dot-dashed, and three-dot-dashed

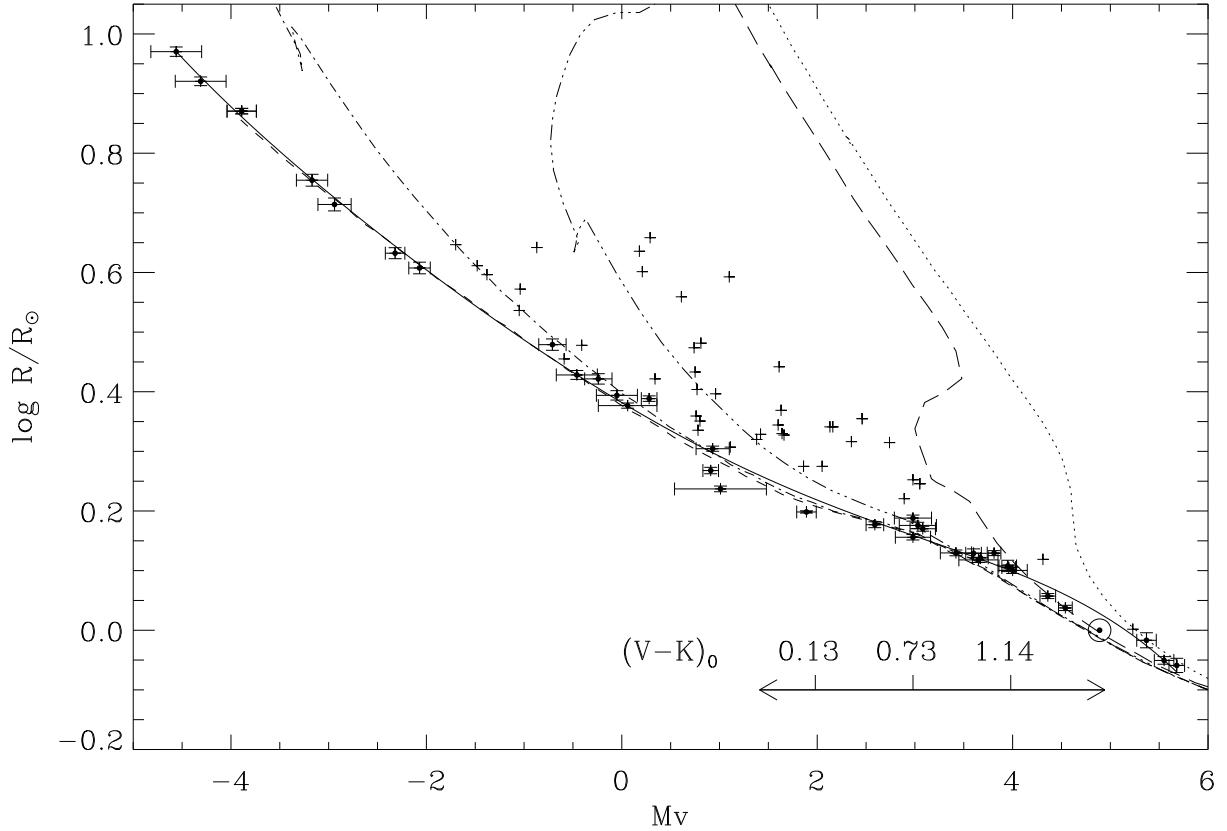


Fig. 2.— Radii vs. absolute visual magnitudes for eclipsing binaries. The crosses have been dismissed as they have already evolved significantly from the ZAMS. The solid line corresponds to a fifth-order polynomial. The dashed, dot-dashed, three-dot-dashed, long-dashed, and dotted lines show isochrones of 4 Myr, and 0.04, 0.4, 4, 20 Gyr, respectively. The arrow marks the range of applicability for the  $S_V - (V - K)_0$  relation.

lines in Figure 2) predict slightly smaller radii for  $M_V > 3$ . The Sun itself, which has been included in the fitting sample, might be slightly smaller than the trend suggested by the immediately cooler and hotter stars. Pols et al. (1997), in a comparison of evolutionary models against eclipsing binaries, found inconsistencies for the systems whose components were close to or below one solar mass – considering the same sample as here. However, these systems are either active binaries or flare stars. The M1 twins in the system YY Gem ( $M_V \simeq 9$ ), and the cool components of RT And and CG Cyg ( $M_V \simeq 6.3$ ) are far from the range of luminosities of interest for this work (namely, where the relationship between  $S_V$  and  $(V - K)_0$  has been tuned, identified in Figure 2 with the arrows) and have been excluded from further consideration, but they fit well in the same picture. The hypothesis that some of these systems are evolving off the main-sequence is not

plausible, as those at  $M_V \simeq 5.5$  mag are expected to freeze in their ZAMS position for a period of time longer than the age of the Galaxy. The fact that the radii observed at a given  $M_V$  is larger than expected at the ZAMS could be induced by the stars undergoing contraction. Alternatively, the disagreement could be related to the stars' membership to binary systems, since models are constructed for isolated (non- interacting) stars. Another symptom of inconsistencies with stellar evolution models has been discussed by Popper (1997) and Clausen et al. (1999): binaries with one component in the mass range  $0.7 - 1.1M_\odot$  do not lie along a unique isochrone. With no definite answers in hand, we adopt the empirical fit, cautioning the reader about possible systematic errors on the cool side of our  $T_{\text{eff}}$  range.

The scatter about the fit is significantly larger than the error bars and, as explained by Andersen (1991), it mostly corresponds to real differences in chemical abundances, age, rotational velocities, etc., among the stars. While the radii compiled by Andersen (1991) are of strictly observational origin, the absolute magnitudes were derived from effective temperatures and bolometric corrections ( $BCs$ ). The effective temperatures were compiled from a number of heterogeneous sources, including broad-band photometry, intermediate-band photometry, and spectrum synthesis, all dependent on model atmospheres. Bolometric corrections depend on model atmospheres too (see Popper 1980 for the details of the scale used by Andersen 1991). These two factors introduce additional noise in defining the relationship in Eq. 3. More importantly, however, is that the zero point of the  $T_{\text{eff}}$  and  $BC$  scales could induce systematic effects in Eq. 3. From the definition of luminosity, we can write  $\sigma^2(\log \frac{L}{L_\odot}) = 4\sigma^2(\log \frac{R}{R_\odot}) + 16\sigma^2(\log \frac{T_{\text{eff}}}{T_\odot})$ . As radii and effective temperatures in Andersen's compilation are typically determined within 2 % and 3-4 %, respectively, the error in the luminosity is dominated by the uncertainty in the effective temperature. Similarly, from the definition of visual and bolometric magnitudes, we can write  $\sigma^2(M_V) = 2.5^2\sigma^2(\log \frac{L}{L_\odot}) + \sigma^2(BC) \simeq 2.5^2 16\sigma^2(\log \frac{T_{\text{eff}}}{T_\odot}) + \sigma^2(BC)$ . Given the expected uncertainties in the  $BCs$  for late-type stars are not expected to be larger than about 0.04 mag, we should only worry about the  $T_{\text{eff}}$  scale, and  $\sigma(M_V) \simeq 4.34 \frac{\sigma(T)}{T}$ . Very recently, Ribas et al. (2000) have critically revised Andersen's  $T_{\text{eff}}$ s. The updated values, mostly on the scale of modern Kurucz's model atmospheres (Kurucz 1991, 1994), are compared with those published by Andersen in Figure 3. The mean difference  $\log T_{\text{eff}}(\text{Andersen}) - \log T_{\text{eff}}(\text{Ribas et al.})$  is  $-0.0014 \pm 0.0013$ , which implies a correction to  $M_V$  of roughly 0.014 mag, suggesting that Andersen's values, and therefore Eq. (1), are not significantly biased.

Ideally, one would estimate  $M_V$  directly from trigonometric parallaxes. *Hipparcos* has observed a number of eclipsing binaries with sufficient accuracy (Popper 1998). Unfortunately, most of the components of those systems have evolved significantly from the ZAMS. It is, however, reassuring that the absolute magnitudes derived by Popper (1998) for the few components that appear on, or very close to the ZAMS are in good agreement with the indirect determinations listed by Andersen (1991).

The relationship between  $\frac{R}{R_\odot}$  and  $M_V$  for stars near the ZAMS in Eq. 3, can be expressed in terms of the parallax, as  $\log p = \frac{1}{5}(M_V - V_0 - 5)$ , where  $V_0$  is the intrinsic V magnitude of the star.

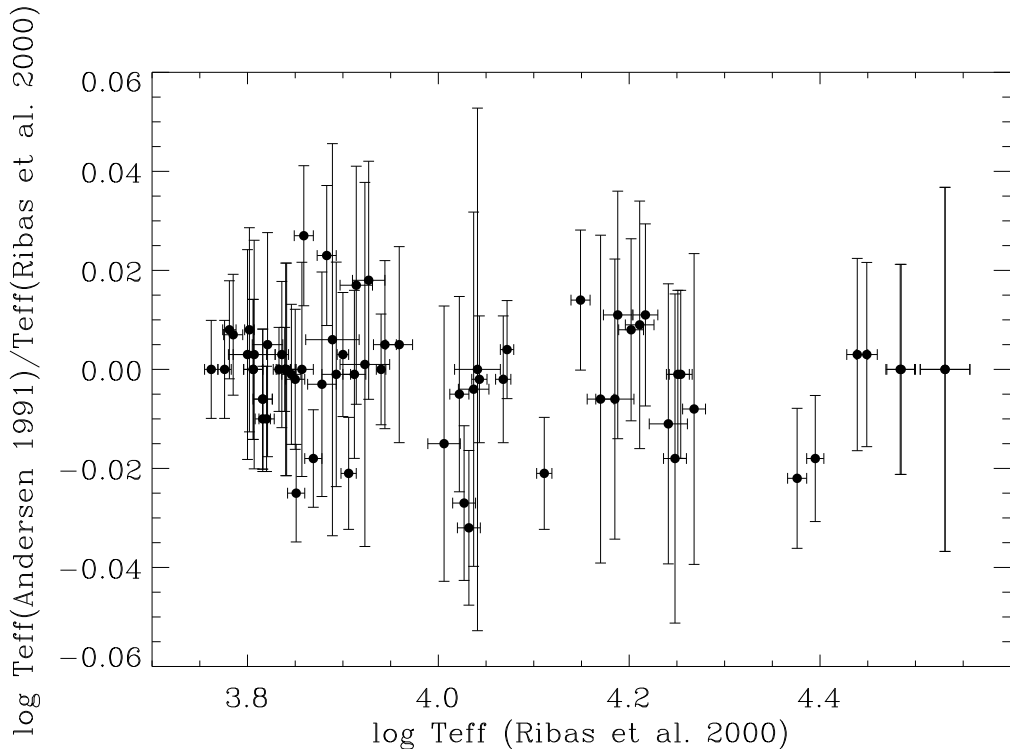


Fig. 3.— Comparison between the effective temperatures used by Andersen (1991) to estimate absolute  $V$  magnitudes, and the recently revised values of Ribas et al. (2000).

Then, the Eqs. 2 and 3 form a complete system of equations that provide  $\frac{R}{R_{\odot}}$  and  $\log p$ , once the  $V_0$  and  $K_0$  intrinsic magnitudes are known.

Eclipsing binaries are a special case. The radii of the components can be determined directly and, using the  $S_V$  vs.  $(V - K)_0$  (or  $S_V - T_{\text{eff}}$ ) relationship to infer the angular diameter, Eq. 2 provides the distance. This recipe will eliminate the need for spectrophotometry, and the prospective error in the angular diameter might be even smaller, as adopting  $\sigma(S_V) \simeq 0.05$ , then  $\sigma(\theta) \simeq 2\%$ . Unfortunately, the only two eclipsing binaries analyzed in the LMC at the time of this writing (Guinan et al. 1998, Ostrov, Lapasset & Morrell 2000) are way hotter than the range covered by Di Benedetto’s  $S_V$  vs.  $(V - K)_0$  fit.

## 2.2. Unknown reddening

The pair of relations between  $\log \frac{R}{R_{\odot}}$  and  $\log p$  (Eqs. 3 and 2) described in the previous subsection requires a third equation to solve for an additional variable, the interstellar reddening. This implies the adoption of a simplified model for the interstellar absorption, assuming that  $\mathcal{R} \equiv A(V)/E(B - V)$  is known ( $\mathcal{R} = 3.1$  is the mean value for the galactic interstellar medium). It

is well-known that  $\mathcal{R}$  does not have a universal value, but instead changes spatially, depending on the absorption and scattering properties of the interstellar medium. There are, however, different ways to derive  $\mathcal{R}$  from empirical determinations of the reddening in different colors (see Fitzpatrick 1999 and references therein).

The  $(B - V)_0$  color index is available for the components of all binaries previously considered, and can be related to the stellar radius. Figure 4, which includes the same stars used to build the  $\log \frac{R}{R_\odot}$  vs.  $M_V$  relationship, shows that the observed radii correlate tightly with the color index, in very good agreement with the ZAMS predicted by the isochrones for  $(B - V)_0 \leq 0.3$  (their code is the same as in Figure 2). Again, the match does not hold for cooler stars. The solid line in Figure 4 corresponds to a fifth-order polynomial, given by:

$$\log \frac{R}{R_\odot} = 2.266 \times 10^{-1} - 5.222 \times 10^{-1}(B - V)_0 + 2.767(B - V)_0^2 - 7.387(B - V)_0^3 + 7.245(B - V)_0^4 - 2.471(B - V)_0^5, \quad (4)$$

which holds between  $-0.3 \leq (B - V)_0 \leq 0.8$ , and shows a standard deviation of 0.03 dex.

This third empirical relationship provides a single value for the stellar radius, once the intrinsic  $(B - V)_0$  color is known. The stellar absorption in the V band,  $A(V)$ , is introduced into the equations through the expressions for the reddening in the two color indices:

$$\begin{aligned} E(B - V) &= \frac{A(V)}{\mathcal{R}} \\ E(V - K) &= A(V) \frac{(\mathcal{R} - 0.02)}{1.12\mathcal{R}} \end{aligned} \quad (5)$$

(Fitzpatrick 1999), and adopting (or measuring) a value for  $\mathcal{R}$ , we have a system of three equations in which  $\log \frac{R}{R_\odot}$ ,  $\log p$ , and  $A(V)$  are the unknowns.

### 2.3. Summary and practical application of the procedure

The procedure to estimate distances can be summarized as follows. When the reddening is known, one can derive the stellar radius and parallax by combining two of the following three equations:



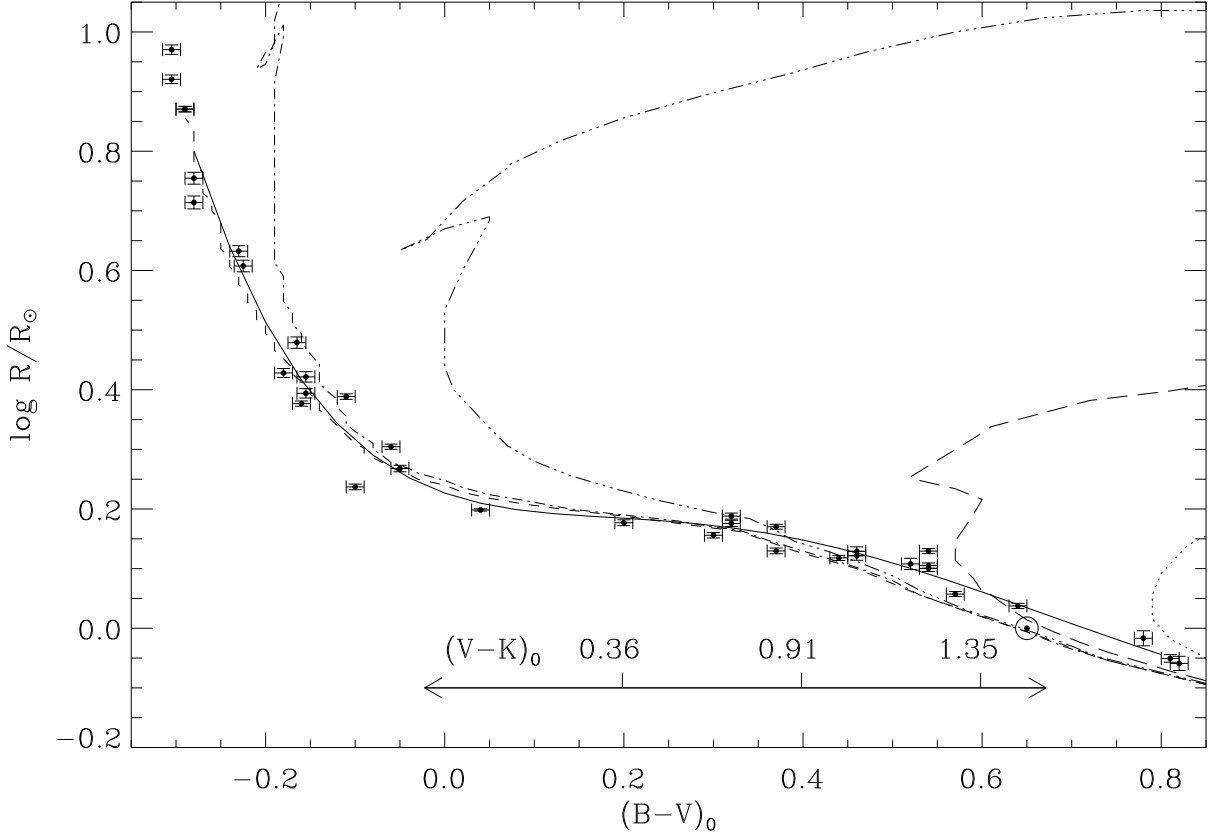


Fig. 4.— Radii vs.  $(B - V)_0$  for eclipsing binaries close to the ZAMS. The solid line represents a fifth-order polynomial and the other curves correspond to isochrones of solar composition and different ages, following the convention of Figure 2.

$$\left\{ \begin{array}{l} \log \frac{R}{R_\odot} = 2.031 + \log \theta - \log p \\ \log \frac{R}{R_\odot} = 3.820 \times 10^{-1} - 9.801 \times 10^{-2} M_V + 7.636 \times 10^{-3} M_V^2 \\ \quad + 4.895 \times 10^{-4} M_V^3 - 6.133 \times 10^{-5} M_V^4 - 2.831 \times 10^{-5} M_V^5 \\ \log \frac{R}{R_\odot} = 2.266 \times 10^{-1} - 5.222 \times 10^{-1} (B - V)_0 + 2.767 (B - V)_0^2 \\ \quad - 7.387 (B - V)_0^3 + 7.245 (B - V)_0^4 - 2.471 (B - V)_0^5, \end{array} \right. \quad (6)$$

where

$$\left\{ \begin{array}{l} \log \theta = \frac{1}{5} (S_V [(V - K)_0] - V_0 - 15) \\ M_V = V_0 + 5 + 5 \log p. \end{array} \right. \quad (7)$$

$BVK$  and  $M_V$  are given in magnitudes,  $\theta$  and  $p$  in arcseconds, and  $S_V [(V - K)_0]$  is in magnitudes,

as prescribed in Eq. 1.

When reddening is unknown, but  $\mathcal{R} \equiv A(V)/E(B - V)$  can be estimated, one should solve simultaneously the three equations in the system (6), where

$$\left\{ \begin{array}{l} \log \theta = \frac{1}{5}(S_V[(V - K)_0] - V_0 - 15) \\ M_V = V_0 + 5 + 5 \log p \\ V_0 = V - A(V) \\ (B - V)_0 = (B - V) - A(V)/\mathcal{R} \\ (V - K)_0 = (V - K) - A(V) \left( \frac{\mathcal{R} - 0.02}{1.12\mathcal{R}} \right). \end{array} \right. \quad (8)$$

The upper panel of Figure 5 shows a graphical example corresponding to the analysis of the star HD 224817 (HIP 80), with  $B = 8.97$ ,  $V = 8.40$  and  $K = 6.92$ . The curves labeled as  $a$ ),  $b$ ) and  $c$ ) correspond to the definition of angular diameter (Eq. 2), the  $\log \frac{R}{R_\odot} - M_V$  (Eq. 3), and the  $\log \frac{R}{R_\odot} - (B - V)_0$  (Eq. 4) relationships, respectively. It has been assumed a null interstellar absorption, a plausible hypothesis for a star at roughly 64 pc from the Sun or, equivalently, with  $\log p = -1.81$ . The crossing points are:  $a - b : -1.77$ ,  $a - c : -1.79$ , and  $b - c : -1.82$ , indicating distances within 10% of that derived from the parallax measured by *Hipparcos*. The power of the suggested procedure will strongly depend on the way each of the three curves responds to changes in the interstellar absorption. The lower panel of Figure 5 shows such variations and, for this particular case, the three crossing points change nearly in parallel against  $A(V)$  – a remarkably odd feature.

To determine whether it is possible or not to extract information on the interstellar reddening, I assume a given distance and amount of reddening and then, make use of Bertelli et al’s ZAMS to estimate the absolute visual magnitude of stars with different  $(V - K)_0$  color. I derive the observed  $V$  magnitude and, via Eqs. 3, 4, and 5, the observed  $B$  and  $K$  magnitudes. Then, I determine the variation with reddening of the parallax at which the three curves in the  $\log \frac{R}{R_\odot} - \log p$  plane cross. Figure 6 shows the variation of the mean value of  $\frac{\partial \log p}{\partial A(V)}$  for the  $a - b$  (solid),  $a - c$  (dashed), and  $b - c$  curves. The error bars correspond to the standard deviation of the slopes of the curves, which are close to, but not quite, straight lines in the vicinity of the right  $A(V)$ . The three lines change in parallel for a star with  $(V - K)_0 \simeq 1.5$ , with a slope of about  $-0.7$ , as confirms Figure 5b, but the slope of the variation of the crossing points  $b - c$  is significantly different from the other two combinations for stars with  $(V - K)_0 \simeq 0.4$  or  $T_{\text{eff}} \simeq 8000$  K. This result suggests that stars with spectral types A3–A6 are suitable for extracting the interstellar reddening.

### 3. A check against *Hipparcos*. Evolution effects

Di Benedetto (1998) compiled  $V$  and  $K$  photometry, and derived empirical effective temperatures for a large number of stars selected as flux standards for the Infrared Space Observatory

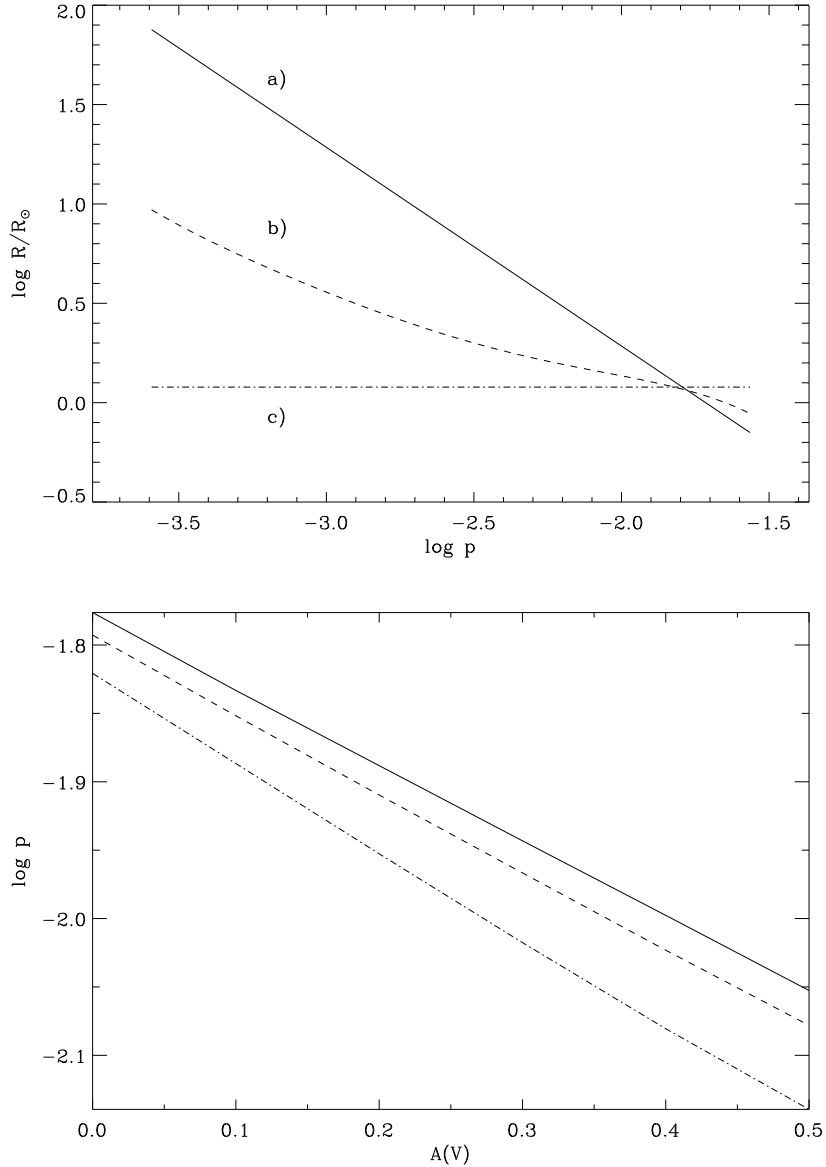


Fig. 5.— *Upper panel:* Lines defined by the  $S_V - (V - K)_0$  (solid line; *a*),  $\log \frac{R}{R_{\odot}} - M_V$  (dashed; *b*), and  $\log \frac{R}{R_{\odot}} - (B - V)_0$  (dot-dashed; *c*) relationships for the star HD 224817. *Lower panel:* Variation of the crossing points between the curves *a* – *b* (solid line), *a* – *c* (dashed), and *b* – *c* (dot-dashed) against  $A(V)$ .

(ISO). A large fraction of them have precise parallaxes measured in the *Hipparcos* catalog, and are considered here for testing the suggested procedure to estimate distances. I have restricted the analysis to the Northern Hemisphere stars classified as dwarfs with errors in the parallax smaller than 30 %. Most of the stars are nearby, and assuming  $A(V) = 0$  is appropriate in most cases.

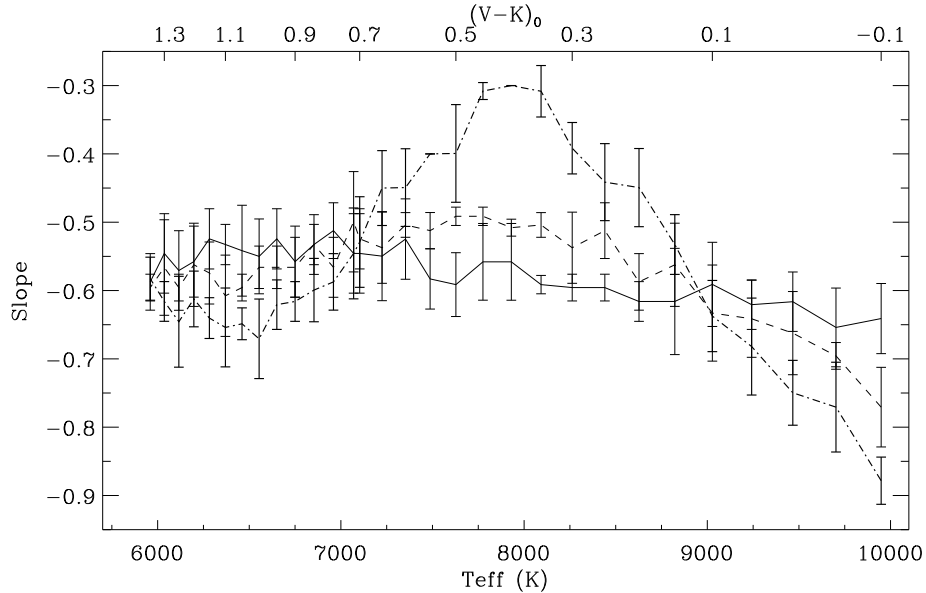


Fig. 6.— Mean slope of the position of the crossing points between each pair of the the  $\log \frac{R}{R_{\odot}}$  vs.  $\log p$  curves:  $a - b$ ,  $a - c$ , and  $b - c$ , for stars of different effective temperatures ( $(V - K)_0$  colors).

As stars evolve away from the ZAMS or, more precisely, from the vicinity of the  $\log \frac{R}{R_{\odot}} - M_V$  and  $\log \frac{R}{R_{\odot}} - (B - V)_0$  lines empirically defined by the components of eclipsing binaries, the use of such relationships will result in underestimated radii or, equivalently, distances. To quantify this effect we can set limits to the luminosity above the ZAMS of the stars analyzed. In practice, when applying the method to stellar clusters, that limit can be set with respect to the lower boundary, in brightness, of the main sequence. An analysis of the HR diagram, mainly the slope of the main sequence band, should reveal if the considered stars have started to depart significantly from the ZAMS.

Figure 7 compares the distances derived from the mean of the crossing points  $a - b$ ,  $a - c$  and  $b - c$ , with those derived from the *Hipparcos* parallaxes, restricting the analysis to stars with absolute visual magnitudes: i) 0.5 mag, ii) 1.0 mag, and iii) 1.5 mag brighter than the theoretical ZAMS. The mean and rms differences between the retrieved distances and those derived from the *Hipparcos* parallaxes for the case i),  $\frac{d(\text{THIS WORK}) - d(\text{HIP})}{d(\text{HIP})}$ , are displayed in Table 1. I have considered the entire sample, as well as several divided subgroups, depending of their effective temperature.

A first and very important remark is that the limits of 0.5, 1.0 and 1.5 magnitudes above the theoretical ZAMS are not affecting equitably stars of different mass. As shown in Figure 4, the observed radii are slightly larger than the isochrones' prediction for stars with  $(B - V)_0 > 0.3$  ( $T_{\text{eff}} \lesssim 7000$  K) by some quantity that can reach up to 0.05 dex. This implies that the chosen

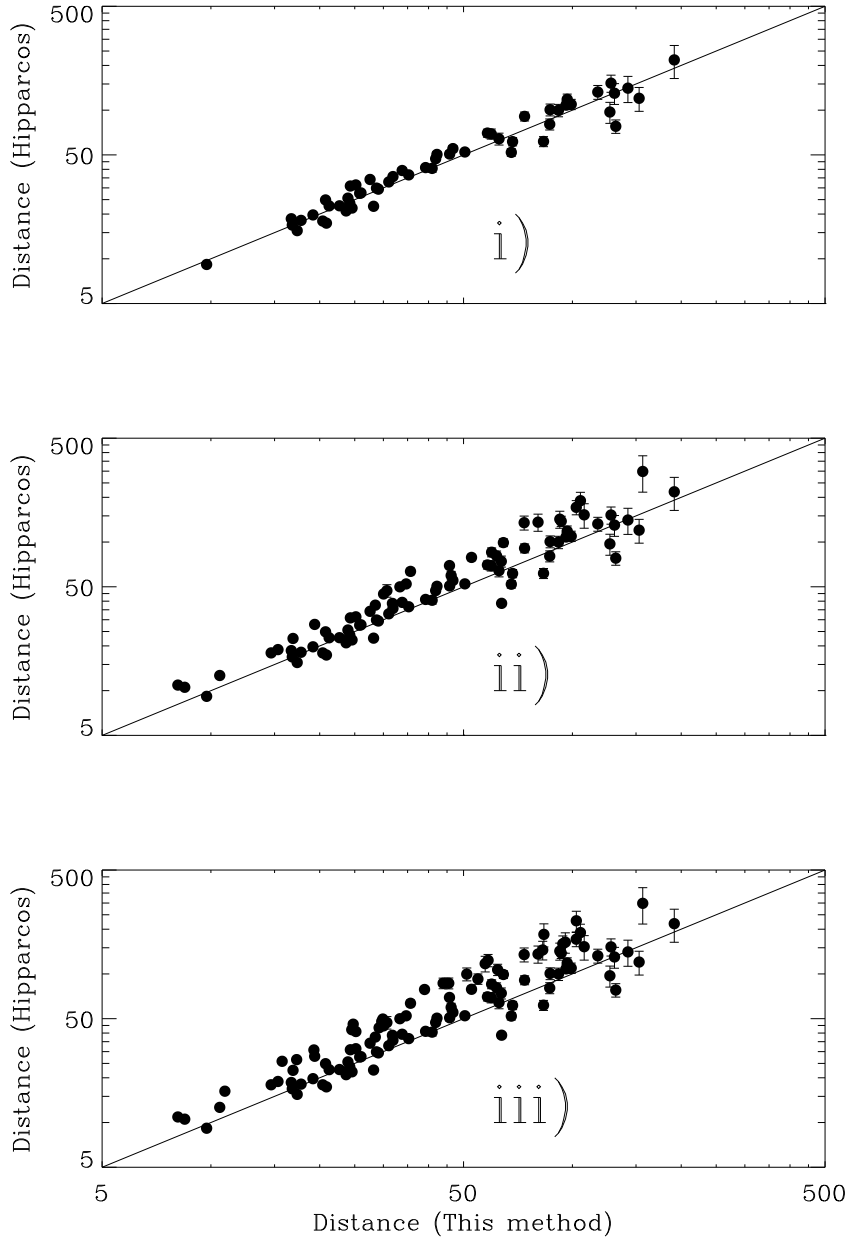


Fig. 7.— Comparison between the retrieved distances and those derived from *Hipparcos* parallaxes when the limiting luminosity is set to 0.5 (i), 1.0 (ii), and 1.5 (iii) mags above the ZAMS predicted by the evolutionary models of Bertelli et al. (1994).

criterion is some 0.2 magnitudes more strict for these stars, which dominate the sample, than for their hotter partners, and therefore we should translate the sequence of 0.5 – 1.0 – 1.5 mag into 0.3 – 0.8 – 1.3 mag. Averaging the results for the crossing points  $a - b$ ,  $a - c$  and  $b - c$ , the mean

difference between the derived and the *Hipparcos* parallaxes (or distances) is  $-1 \pm 2$  %. Using any single crossing point the systematic difference is never larger than 5%, and restricting the comparison to stars with effective temperatures lower than 7000 K, which constitute more than three quarters of the sample, similar results hold. The twelve stars with  $\geq 7000$  K show a systematic departure from the *Hipparcos* measurements. This is likely the result of evolutionary effects. After a few Gyr these stars are no longer expected to be near the ZAMS (see the three-dot-dashed line in Fig. 2). Finally, it is of interest to mention that if we derive a relationship between  $M_V$  and  $(B - V)_0$  for the components of eclipsing binaries and we use it to determine photometric parallaxes for the same *Hipparcos* sample, the retrieved distances would have an uncertainty that is roughly 50 % larger.

#### 4. Metallicity effects

We recall that the  $S_V - (V - K)_0$  relationship is expected to be extremely independent of the metal abundances, but the proposed procedure involves two other relations that are not. A strong dependence on metallicity would be very negative, for the sample of eclipsing binaries have metal abundances not far from solar, and they constitute the only empirical resource considered. The ZAMS isochrone for solar metallicity departs from the preferred empirical relationships for stars cooler than 7000 K, but at  $M_V = 3.16$  ( $(B - V)_0 = 0.25$ ), where the curves have an inflection point, their agreement is perfect. We can make use of that reference to estimate the systematics in case the metal abundance happens to differ from solar.

Figure 8 shows the empirical relations between  $\log \frac{R}{R_\odot}$  and  $M_V$  or  $(B - V)_0$  (solid line) and the predictions of the isochrones (dashed line) for solar abundances as well as differences in defect and excess by 0.4 dex. The empirical relations have been scaled as well, adopting the relative shape between models of different metal content, to produce the uppermost (larger radii) and lowermost (smaller radii) solid curves. At the inflection point, for the two relationships, the changes in radius are very close to linear all the way down to  $\log \frac{Z}{Z_\odot} = -2$ , and probably below that, with a positive slope slightly smaller than 0.1 dex per dex. Combining this result with Eq. 2, we can directly translate that to a systematic effect upon the derived distance. In short, the effect is quite small for moderate departures from solar metallicity. For instance, ignoring the fact that a star is about  $-0.2$  dex metal deficient compared to the Sun will not introduce a systematic error larger than a 5%, in the sense that the distance will be overestimated.

#### 5. Summary and discussion

This paper describes a new method to determine distances to unevolved stars. The errors involved in the practical application to individual stars are relatively large ( $\sim 15$  %), but the procedure is still of great interest when applied to clusters. It is based on empirical relationships,

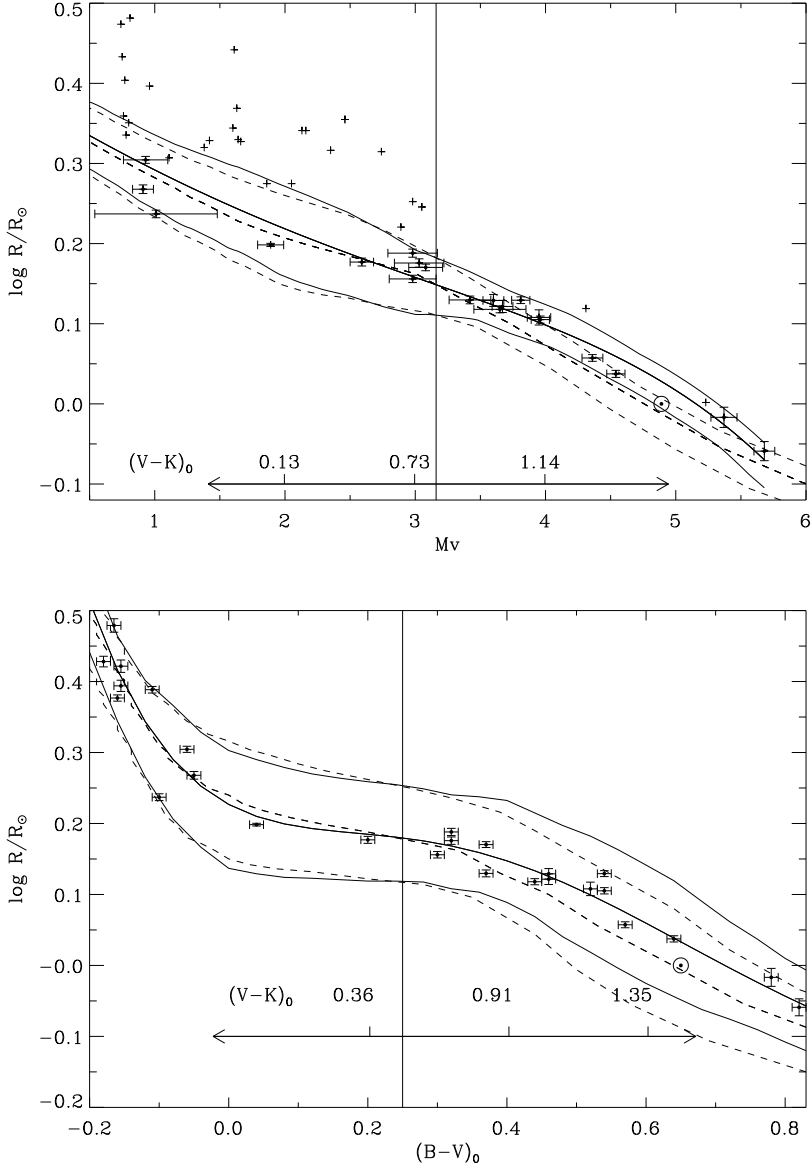


Fig. 8.— Relationships between  $\log \frac{R}{R_{\odot}}$  vs.  $M_V$  or  $(B - V)_0$  for  $\log \frac{Z}{Z_{\odot}} = -0.4, 0,$  and  $0.4$ , as predicted by the isochrones (dashed lines), or from the polynomial fitted to the eclipsing binaries (of roughly solar composition), scaled with the shape predicted by the isochrones (solid lines). At the inflection points (solid vertical lines), a change of 0.1 dex per dex is observed.

although model atmospheres enter to define a) a limb-darkening law for obtaining true angular diameters from observations, and b)  $T_{\text{eff}}$  and  $BC$ , providing  $M_V$ . The method takes advantage of direct determinations of radii in eclipsing binaries to establish relationships between radius and absolute visual magnitude and radius and  $(B - V)_0$  color. It benefits from the solid Barnes-

Evans like correlation existing between surface brightness,  $S_V$ , and the  $(V - K)_0$  color index or, equivalently, between the latter and the stellar angular diameter.

The procedure, which only makes use of *BVK* photometry, can be applied without modification to estimate distances to stellar systems with known reddening, and with a chemical composition close to solar. It requires the target stars, dwarfs with effective temperatures between 6000 and 10000 K, not to have evolved significantly from the ZAMS, and therefore, it is restricted to systems with ages up to 2 Gyr, approximately. Unevolved dwarfs with effective temperatures close to 8000 K ( $0.3 \lesssim (V - K)_0 \lesssim 0.5$ ), can be used to constrain the reddening under the assumption that  $\mathcal{R} \equiv A(V)/E(B - V)$  is known (maybe adopting the mean value for the galactic interstellar medium, 3.1).

Eclipsing binaries including unevolved stars with  $6000 \leq T_{\text{eff}} \leq 10000$  K are a particular case where extremely reliable distances can be derived, independently from bolometric corrections and without spectrophotometry.

Assuming an LMC distance modulus of 18.7, the stars of interest would have magnitudes of  $20.2 \lesssim V \lesssim 23.7$ , right at the edge of current capabilities (see, e.g., Brandner et al. 1999). Besides, many galactic clusters constitute appropriate targets for this method, although no complete *BVK* observations of large numbers of stars in any young open cluster have been published so far. Further improvements can be expected if *K* magnitudes and spectroscopic metallicities become available for the components of eclipsing binaries. The acquisition, careful analysis, and reduction to individual color indices of infrared light curves for eclipsing binaries is very desirable. That would make it possible to extend, and improve, the relationships between fundamental stellar properties and the colors employed here.

I thank David Lambert, Barbara McArthur, Jocelyn Tomkin, and Russel White for comments and discussions. Constructive criticism from the referee, Ignasi Ribas, helped to improve the paper.

## REFERENCES

- Andersen, J. 1991, *ARA&A*, 3, 91
- Barnes, T. G., & Evans, D. S. 1976, *MNRAS*, 174, 489
- Bertelli, G., Bressan, A., Chiosi, C., Fagotto, F., & Nasi, E. 1994, *A&AS*, 106, 275
- Brandner, W., Grebel, E. K., Zinnecker, H., & Brandl, B. 1999, in *New Views of the Magellanic Clouds*, IAU Symp. 190, Y.-H. Chu, N. B. Suntzeff, J. E. Hesser, and D. A. Bohlender, eds., (ASP: San Francisco) p. 366
- Clausen, J. V., Baraffe, I., Claret, A., & Vandenberg, D. A. 1999, in *Stellar Structure: Theory and*



- Test of Convective Energy Transport, A. Giménez, E. F. Guinan and B. Montesinos, eds., ASP Conf. Series, Vol. 173, (ASP: San Francisco) p. 265
- Di Benedetto, G. P., 1998, *A&A*, 339, 858
- ESA 1997, The Hipparcos and Tycho Catalogues, ESA SP-1200
- Feast, M. 1999, in *New Views of the Magellanic Clouds*, IAU Symp. 190, Y.-H. Chu, N. B. Suntzeff, J. E. Hesser, and D. A. Bohlender, eds., (ASP: San Francisco) p. 542
- Fitzpatrick, E. L. 1999, *PASP*, 111, 63
- Guinan, E. F., Fitzpatrick, E. L., Dwarf, L. E., Maloney, F. P., Maurone, P. A., Ribas, I., Pritchard, J. D., Bradstreet, D. H., & Giménez, A. 1998, *ApJ*, 509, L21
- McArthur, B. E., Benedict, G. F., Lee, J., Lu, C.-L., van Altena, W. F., Deliyannis, C. P., Girard, T., Fredrick, L. W., Nelan, E., Duncombe, R. L., Hemenway, P. E., Jefferys, W. H., Shelus, P. J., Franz, O. G., & Wasserman, L. H. 1999, *ApJ*, 520, L59
- Mould, J. R. et al. 2000, *ApJ*, 529, 786
- Ostrov, P. G., Lapasset, E., & Morrell, N. I. 2000, *A&A*, in press (astro-ph/0003118)
- Pinsonneault, M. H., Stauffer, J. Soderblom, D. R., King, J. R., & Hanson, R. B. 1998, *ApJ*, 504, 170
- Pols, O. R., Tout, C. A., Schröder, K.-P., Eggleton, P. P., & Manners, J. 1997, *MNRAS*, 289, 869
- Popper, D. M. 1980, *ARA&A*, 18, 115
- Popper, D. M. 1994, *AJ*, 103, 1091
- Popper, D. M. 1997, *AJ*, 114, 1195
- Popper, D. M. 1998, *PASP*, 110, 929
- Reed, B. C. & Reed, L. G. 2000, *PASP*, 112, 409
- Ribas, I., Giménez, A., Torra, J., Jordi, C., & Oblak, E. 1998, *A&A*, 330, 600
- Ribas, I., Jordi, C., Torra, J., & Giménez, A., E. 2000, *MNRAS*, 313, 99
- Robichon, N., Arenou, F., Mermilliod, J.-C., & Turon, C. 1999, *A&A*, 345, 471
- Rosenberg, A., Saviane, I., Piotto, G., & Aparicio, A. 1999, *AJ*, 118, 2306
- van Belle, G. T. 1999, *PASP*, 111, 1515
- Wesselink, A. J. 1969, *MNRAS*, 144, 297

Table 1. Relative mean (and standard deviation) between the retrieved distances and those derived from *Hipparcos* parallaxes.

Sample	$a - b$	$a - c$	$b - c$	Average	N
All	-0.05 (0.13)	-0.02 (0.15)	0.04 (0.26)	-0.01 (0.17)	55
$T_{\text{eff}} < 7000$	-0.03 (0.14)	0.01 (0.15)	0.11 (0.25)	0.03 (0.17)	43
$7000 \leq T_{\text{eff}} < 8000$	-0.18 (0.05)	-0.16 (0.06)	-0.11 (0.09)	-0.15 (0.07)	3
$8000 \leq T_{\text{eff}} < 9000$	-0.13 (0.02)	-0.15 (0.02)	-0.18 (0.07)	-0.15 (0.03)	4
$T_{\text{eff}} \geq 9000$	-0.07 (0.04)	-0.14 (0.04)	-0.26 (0.04)	-0.16 (0.04)	5